[Article ID] 1003- 6326(2001)06- 0965- 07

Coordination and bond properties of Al and Si ions in system of Al_2O_3-SiO_2 melts①

WU Yong-quan(吴永全), HOU Huai-yu(侯怀宇), CHEN Hui(陈 辉),
YOU Jing-lin(尤静林), JIANG Guo-chang(蒋国昌)
(Shanghai Enhanced Laboratory of Ferro-Metallurgy, Shanghai University,
Shanghai 200072, P. R. China)

[Abstract] The coordination and bond properties of aluminium and silicon ions were discussed by means of molecular dynamics simulation. By combining KA and MATSUMIYA potentials, the results of simulations agree better with the experiments. Trend of coordination and bond properties changing along with the increasing content Al_2O_3 from 0 to 100% (mole fraction) was obtained. Average bond lengths of Si-O in these simulations are within the range of 1.60~ 1.63 Å and become smaller from 1.63 Å in sample 0 to 1.60 Å in sample 9 along with increasing content of Al_2O_3. Average bond lengths of Al-O are within the range from 1.77 Å in sample 1 to 1.86 Å in sample 10. By analyzing the relation of CN(T) and CNSi(T) with Si/(Si+ Al), it is found that Al mainly locates on the tetrahedral sites which neighbor the Si tetrahedra but avoid the Al tetrahedra while alumina content is low. Whereas when Si/(Si+ Al) < 0.5, Al-octahedral units appeared and became predominant gradually. Meanwhile, Al avoidance principle can only be maintained at low alumina content. With increasing alumina, this principle would be broken gradually.

[Key words] Al_2O_3-SiO_2 melts; coordination and bond properties; molecular dynamics simulation
[CLC number] O 645; O 552.41; TF 01 [Document code] A

1 INTRODUCTION

The properties of binary slag system of Al_2O_3-SiO_2 are basic background knowledge for metallurgist. But up to now, the most majority of knowledge about slag is still based on experience. In order to systemize and theorize the knowledge of properties of slag, complete and further understanding of molten structure of silicate must be the first step because any macroscopic properties of any melts are determined by microstructure. Fortunately, various experimental methods for studying the microstructure of silicate melts have been developed, such as Raman and Infrared spectroscopy[1~4], X-ray photoelectron spectroscopy (XPS)[5], nuclear magnetic resonance (NMR)[4,6~10] and X-ray scattering[11,12]. Parallel to the experimental methods, theoretical calculation and simulation methods, like molecular dynamics simulation (MD), Monte Carlo method (MC), and *ab initio* calculation, have also been developed accompanying with the development of computer, specially MD simulation[11,13~19].

For the structural properties of Al_2O_3-SiO_2 melts, there existed several viewpoints sustained or contradictory with each other in the previous literatures. Mysen, McMillan and Daniel[1~4] studied the aluminosilicate melts by means of Raman and IR spectroscopy and concluded that the aluminum avoidance principle[20] is basically maintained in most aluminosilicate melts or glasses. With increasing Al_2O_3 content, proportion of Al(Ⅴ) (aluminum with 5 coordinate oxygen) and Al(Ⅵ) species is increased. Based on observed Raman bands, McMillan et al[2] went so far as to suggest that the Raman bands in high-frequency (800~ 1 200 cm^{-1}) region are due to vibrations with a predominant character of silicon-oxygen stretching, with aluminum acting only as a perturbation on these. That's to say, these vibrations are not stretching modes of coupled (Si, Al)-O systems, but rather Si-O stretching motions modified by Al^{3+} as a cation coordinating the oxygen, similar to alkali and alkaline earth cations in simple binary silicate glasses. Miura et al[5] analyzed three O 1s signal components of X-ray photoelectron spectroscopy, which are ascribed to non-bridging oxygen (NBO) and two bridging oxygen Si-O-Si, Si-O-Al respectively, and proved that Si and Al existed as tetrahedral but not octahedral cations. Merzbacher et al[6] investigated the abundance of chain-(Q^2), sheet-(Q^3), and framework-like (Q^4) tetrahedral units, and the distribution of Al among those units in CaO (and MgO)-Al_2O_3-SiO_2 glasses by ^{29}Si and ^{27}Al MAS-NMR. And distinct conclusions were obtained: 1) the higher the ratio of Al/(Al+ Si) is, the more Q^3 units and fewer Q^2 and Q^4 units are present in melts; 2) the low charge density of K^+, Na^+ and even Li^+ are not sufficient to stabilize Si tetrahedra with both

① [Foundation item] Project (59832080, 59874016) supported by the National Natural Science Foundation of China
[Received date] 2000- 12- 25; [Accepted date] 2001- 05- 16

an NBO and neighboring Al. Therefore, Al preferentially goes into Q^4 sites and NBOs are 'concentrated', forming Q^2 sites. However, the higher field strength Mg^{2+} and Ca^{2+} ions can more effectively compete with Al for oxygen and well stabilize Q^3 Si tetrahedra with neighboring Al. Based on the similar viewpoint, Engelhardt and Nofz et al[7~9] proposed a Q_m^n (where m is the total number of bridging oxygen atoms and n the number of Al atoms) groups model built up from groups consisting of a central SiO_4 tetrahedron and its directly connected Si or Al atoms, with Ca^{2+} for charge compensation. In the work of Oestrike et al[10] only ^{27}Al signal for Al(Ⅳ) was detected and there was no signal for Al(Ⅵ) in a very wide range of the ratio of Si to Si+Al in aluminosilicate glasses. So, a strong conclusion was reached that there was no Al-octahedral unit in the sodium aluminosilicate glasses, which is opposite to the results of Poe and McMillan[2,4]. Oestrike et al also calculated the mean Si-O bond length per tetrahedron at about 1.60±0.01 and a range of about 1.56~1.66 Å from ^{29}Si signal. Himmel et al[11] studied the structure of calcium aluminosilicate by means of wide-angle X-ray scattering and proved the well-known short-range order of (Si, Al)-tetrahedra by the average atomic distances at 0.165~0.167 nm, 0.265~0.267 nm and 0.309~0.312 nm (T-O, O-O, T-T distances). Himmel also reached two striking conclusions: 1) the structure is built by completely interconnected $TO_{4/2}$-tetrahedra (T=Si, Al) and Ca^{2+} cations located in the vicinity of the distribution of the Al^{3+} $O_{4/2}^{2-}$-tetrahedra for charge balancing. The distribution of the T-O-T bond angle is broad and asymmetric; 2) the alternating order of (Si, Al)-tetrahedra is interrupted, which is contradictory to the aluminum avoidance principle to a certain extent. MORIKAWA et al[12] made use of X-ray scattering intensity data to lead to a conclusion that the average (Si, Al)-O distance varied from 0.161 to 0.179 nm and the average coordination number of O around T(Si, Al) varied from 4.3 to 4.5 following with increasing mass fraction of Al_2O_3 from 0 to 60%. The notable conclusion of the paper is that the short-range structure of the Al_2O_3-rich glass is similar to that of mullite: the average (Si, Al)-O distance is 0.181 nm and the coordination number is 4.7. Hanada and Soga[21] examined the coordination behavior of Si and Al in SiO_2-Al_2O_3 amorphous films synthesized by radio frequency sputtering, via Si and Al K_α and Al K_β X-ray emission spectroscopy. The Si K_α chemical shift was independent of composition, and remained close to the value for vitreous SiO_2 throughout the entire composition range, suggesting that the Si sites remained tetrahedral in these samples.

In order to understand what role aluminum act as in the Al_2O_3-SiO_2 melt system on earth, the change of coordination and bond properties of the melts along with the entire composition must be studied. But limited to the experimental and environmental conditions, almost all the experiments mentioned above didn't cover the entire range of composition with the content of Al_2O_3 varying from 0 to 100% (mole fraction). As a very successful method for simulating silicate structure, molecular dynamics (MD) can remove the stones lying across the experimental process. In this paper, the main purpose is to study the coordination and bond characters of aluminum and silicon through the entire composition of the binary aluminum silicate melts. After that, the next paper will discuss the type of basic units and their distribution. But before all of these, the choice of potential parameters must be accomplished to obtain the best and closest to reality the results of simulations.

2 SIMULATION METHOD

For the molecular dynamics simulations of silicate melts, the choice of potential is the most important one among several major factors[13]. A pair ionic potential of Born-Mayer-Higgins form, which was transformed from the simulation of halides, was successfully used to silicate melts and glasses[14~19]:

$$u(r_{ij}) = q_i q_j / r_{ij} + B_{ij}\exp(-r_{ij}/\rho_{ij}) \quad (1)$$

where $u(r_{ij})$ is the interatomic pair potential and r_{ij} denotes the interatomic distance. The first term in the right hand side represents Coulombic interaction and the second term represents inter-core short-range repulsion interaction. For the parameter of B_{ij} and ρ_{ij}, it is needed to discuss carefully. Refs. [4, 15] used the same copy of potential in Ref. [13], but the ion size parameter of σ_{Si} has two different values of 1.131 Å from Ref. [4, 16] and 1.31 Å from Ref. [14]. As the author's presume, the value of 1.131 Å is a print error, because the distance of Si-O bond in the simulation with this value is about 1.71 Å but the coordination number of oxygen around silicon still remained about 4. The distance seems too large for the Si tetrahedra, but more fit for the Si octahedra. Based on the assuming that σ_{Si}= 1.31 Å, comparison of different potentials have been done before the simulations to obtain the ideal potential and the results of $u_{Si\text{-}O}(r)$ are shown in Fig. 1(a). Here, only two potentials were included for comparison, KA potential[13] and MATSUMIYA potential[17] (both potentials are BMH forms). With the parameters of KA potential, the Si-tetrahedral units in the simulation seem too soft just like the coordination number $N_{Si\text{-}O}(r)$ shown in the Fig. 1(b), but the parameters of MATSUMIYA potential can rigidify the Si-tetrahedral units and make up for the imperfect of KA po-

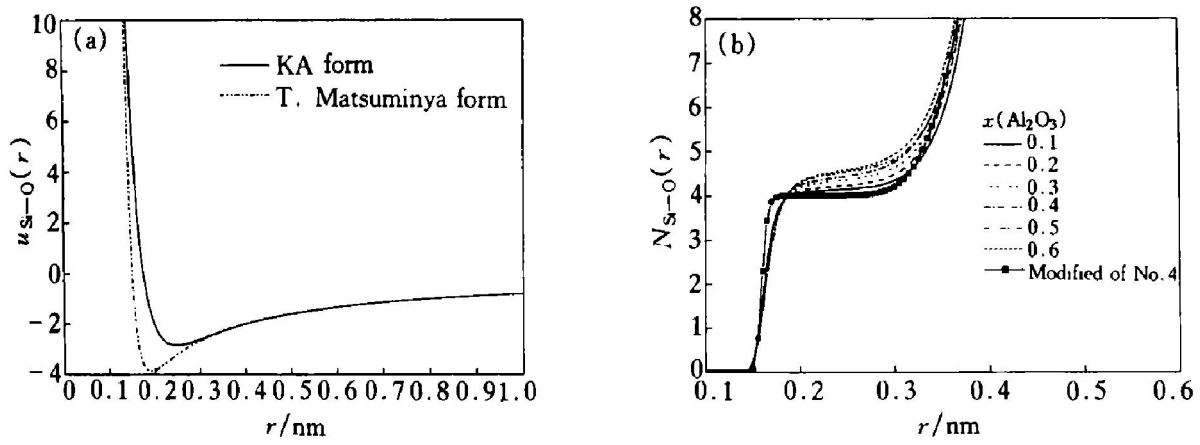

Fig. 1 Comparison of different potentials

tential even as the symbol+ line curve (which simulated the sample 4, see Table 2) of Fig. 1(b), but why? From Fig. 1(a), one can find that the well of MATSUMIYA potential is deeper than that of KA potential, so the attraction between silicon and oxygen of MATSUMIYA potential should be stronger than that of KA potential and therefore Si-tetrahedral units become more rigid. From those comparisons, the combination of two type potentials was applied as listed in Table 1. The ionic valancies q_i for Si, O, and Al are + 4, − 2, and + 3 respectively.

Table 1 Parameters for BMH potential

Bond	ρ_{ij}/ Å	B_{ij}/ eV
Si-Si	0.025	18 660 220 510 030 682 345.0
Si-O	0.142 5	223 440.54
Si-Al	0.29	2 219.246
O-Al	0.29	1 945.759
Al-Al	0.29	2 444.136
O-O	0.260	15 812.842

Table 2 Numbers of atoms and composition of melts

No.	Density /(g·cm^{-3})	$x(Al_2O_3)$ /%	Al	Si	O	Σ(Al+ Si+ O)
0	2.175	0	0	224	448	672
1	2.267	10	42	189	441	672
2	2.355	20	78	159	435	672
3	2.444	30	112	131	430	673
4	4.532	40	142	106	425	673
5	2.621	50	168	84	420	672
6	2.710	60	192	64	416	672
7	2.796	70	214	46	413	673
8	2.885	80	234	29	409	672
9	2.974	90	452	14	406	672
10	3.062	100	268	0	402	670

Note: according to phase diagram[22], liquid region at 2 100 ℃ is across entire region of composition.

In this simulation of the melts, 672 or 673 atoms were included, and the initial construction is random which is most befitting for the simulation of melts and liquids. To make the results more comparable with the results of experiments, the densities are obtained or extrapolated from the experimental data.

The model box lengths will change slightly according to the proportion of Al_2O_3 under the periodic boundary condition. The initial temperature is fixed at 6 000 K for 2000 steps to mix the system completely. Then equilibrium calculation is started and persisted for 8000 steps to reach the required temperature of 2 100 ℃. After equilibrium calculation, the system is relaxed for 5000 steps to discover the RDFs and correlation functions. So the total step number is 15 000, and the time step is 0.002 ps. As mentioned in previous section, the aim of this paper is to detect the coordination and bond properties change caused by increasing Al_2O_3 in the binary melt. So the numbers of Si, O, and Al and the macro-compositions of melt would vary under the condition that the total atom numbers be fixed around 672~ 673. The densities, atom numbers and the compositions are listed in Table 2.

3 RESULTS AND DISCUSSION

RDFs (Radial Distribution Function)[22], acted as a bridge between simulation and experiment, have also been attained in these simulations and compared with X-ray experiments to test the reliability of simulation results. Fig. 2 has shown the RDF results (to avoid the repetition and prolixity, only four samples were selected to show the main feature of simulated RDFs). From Fig. 2, the Si-tetrahedral units must be very rigid because the first peak of $g_{Si-O}(r)$ is very narrow and sharp. That's to say, the aluminum silicate melts inherit the stable short-range order feature of silica melt as shown in Fig. 1(a) to a certain extent.

The average distances of Si-O in these simula-

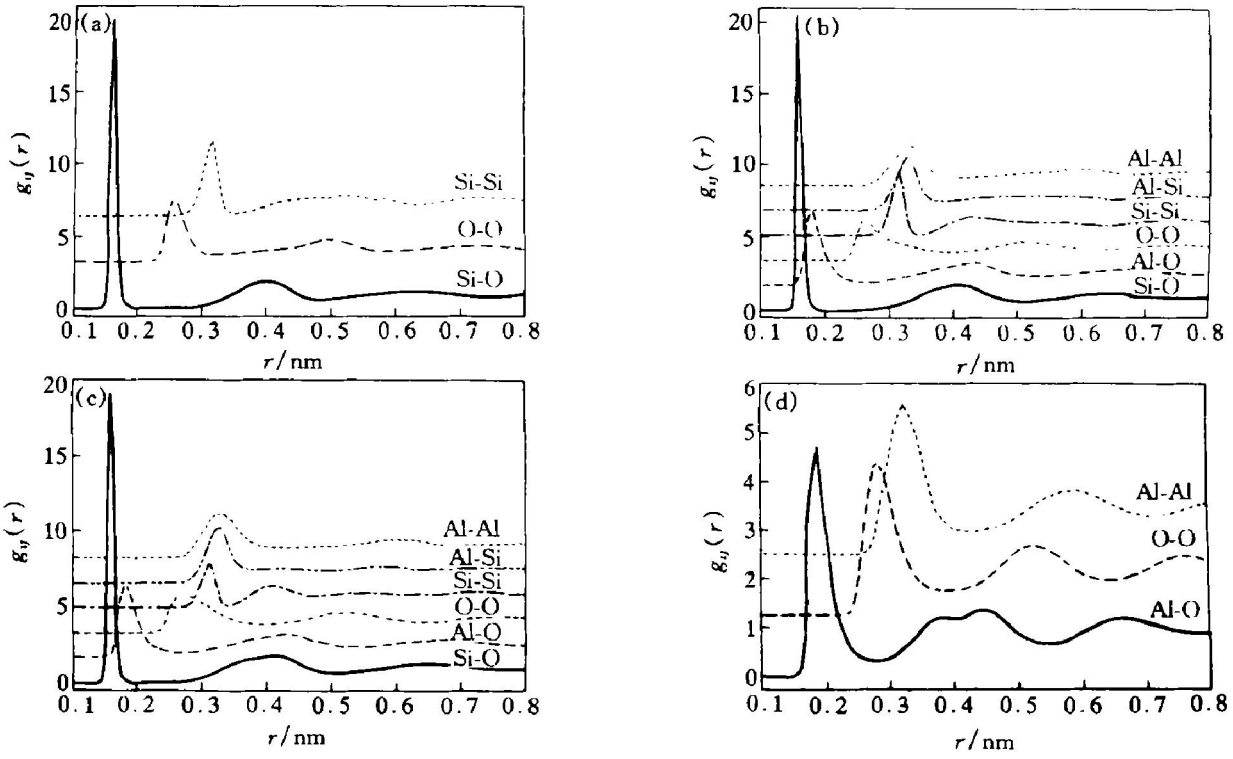

Fig. 2 RDFs of simulation at different mole fraction of Al_2O_3
(a) —$x(Al_2O_3)$ = 0; (b) —$x(Al_2O_3)$ = 40%; (c) —$x(Al_2O_3)$ = 60%; (d) —$x(Al_2O_3)$ = 100%

tions are within the range of 1.60~ 1.63 Å and become smaller from 1.63 Å in sample 0 to 1.60 Å in sample 9 with increasing content of Al_2O_3 as shown in Fig. 3(a), which agrees very well with that of wide angle X-ray scattering experiment[10] (1.615 ± 0.026 Å for anorthite) and NMR data[9] (1.56 ~ 1.66 Å for Si-O bond). The average distances of Al-O are within the range from 1.77 Å in sample 1 to 1.86 Å in sample 10 as shown in Fig. 3(b), which are in agreement with data from Himmel et al[10] (1.749 ±0.033 Å for anorthite and 1.81 Å for mullite) and X-ray scattering intensity data[11] (average distance of (Si, Al)-O is from 1.61 to 1.79 Å for the different content of Al_2O_3 from 0 to 60%). The first peaks of $g_{O\text{-}O}(r)$ shift from 2.60 Å in SiO_2 melt to 2.85 Å in Al_2O_3 melt (agree well with the wide angle X-ray scattering data[10]) and in general compose a peak (ascribed to the O-O pair in Si-tetrahedral units by comparing with that of SiO_2) and a shoulder (ascribed to the O-O pair in Al-tetrahedral units by comparing with that of Al_2O_3) as shown in the Fig. 3(c).

The next-nearest orders are exhibited from the second peaks of $g_{Si\text{-}O}(r)$, $g_{Al\text{-}O}(r)$ and $g_{O\text{-}O}(r)$, but no for $g_{Al\text{-}Si}(r)$. Meanwhile, the positions of first peaks of $g_{Al\text{-}Si}(r)$ are striking identical with each other, 3.28 Å This phenomenon embodied the character of short-range order in Si-O units and Al-O units (tetrahedra or octahedra) and mid- or long-range disorder in melts, at the same time, it interpreted the rationality of the Q_m^n groups model proposed by Engelhardt and Nofz[6~8] to a certain extent. In the binary Al_2O_3-SiO_2 melts, stably existed units should be larger than Q^i which is regarded as stable units in MO-SiO_2 melt system[1~3] (M represents the alkaline earth metals).

The trends of distances of atoms changing with the increasing content of Al_2O_3 can only be interpreted on conditions of integrating with the trends of coordination number curves as shown in Fig. 4. Similar to the alkaline earth silicate melts, coordination numbers curves of Si shown in Fig. 4(a) have a common platform with the y-axis value equal to 4. Combining with the positions of first peaks in Fig. 3(a) and Fig. 4(a), conclusions can be reached with the joining of Al_2O_3, the repulsion of Al to the bridging oxygen of the form Al-O-Si and consequently compression brought to the Si-tetrahedra by NNN (next-nearest neighbor) Al become stronger, so the average distance of Si-O become smaller. Similar to the $N_{Si\text{-}O}(r)$ and $N_{Si\text{-}Si}(r)$ curves, the curves of $N_{Al\text{-}O}(r)$ and $N_{Al\text{-}Si}(r)$ have also platforms just with a little inclination. This character proved the short-range order of $Al \overset{\rightarrow}{} O \overset{\rightarrow}{} Si$ structual units similar to but less rigid than that of $Si \overset{\rightarrow}{} O \overset{\rightarrow}{} T$(Si, Al) structural units. The CN(Al) (the coordination number of O about Al, equal to the value of $N_{Al\text{-}O}(r_0)$, where r_0 represents the position of first min of $g_{Al\text{-}O}(r)$) increases from 3.5 in sample 1 to 5.36 in sample 10 and equal to 3.977 (near 4) at sample 3. The relations of CN(Si) and CN(Al) with Si/(Si+ Al) have been abstracted from the $N_{T\text{-}O}(r)$ and shown in Fig. 5(a).

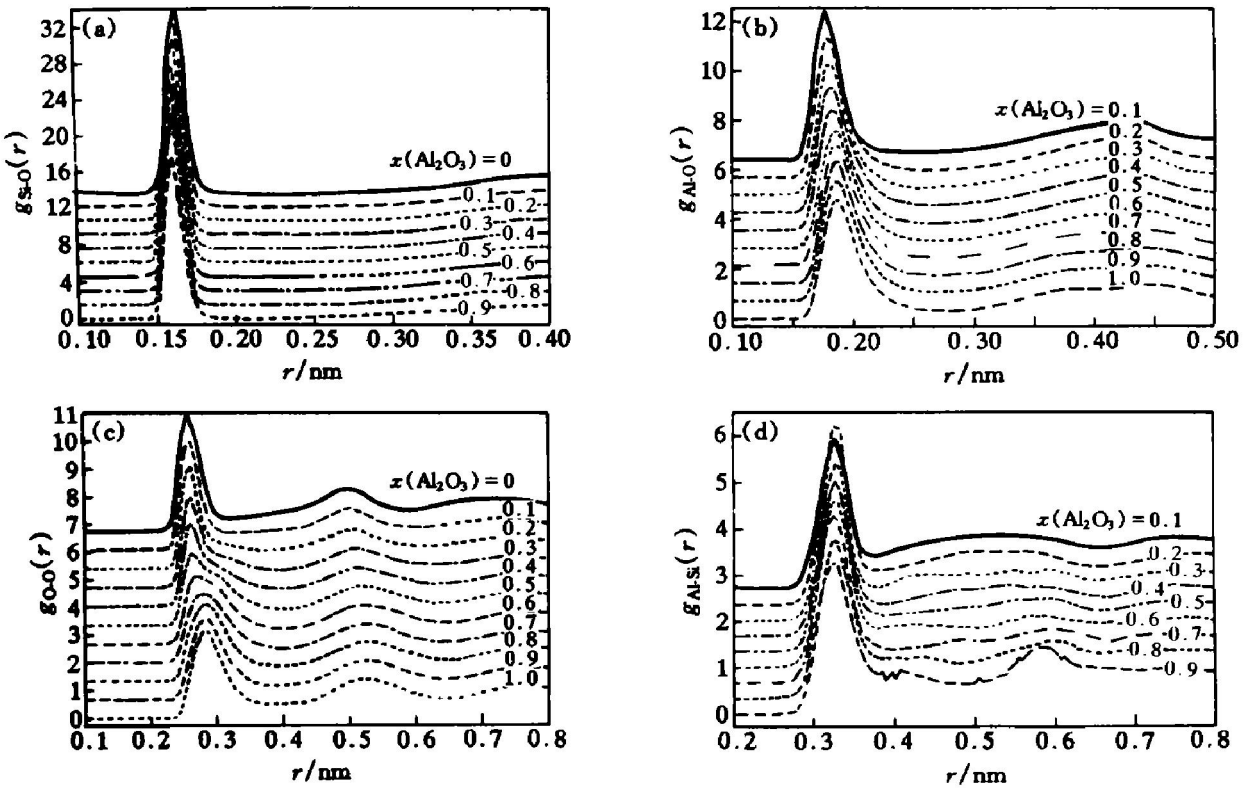

Fig. 3 RDFs of Si-O (a), Al-O (b), O-O (c), and Al-Si (d)

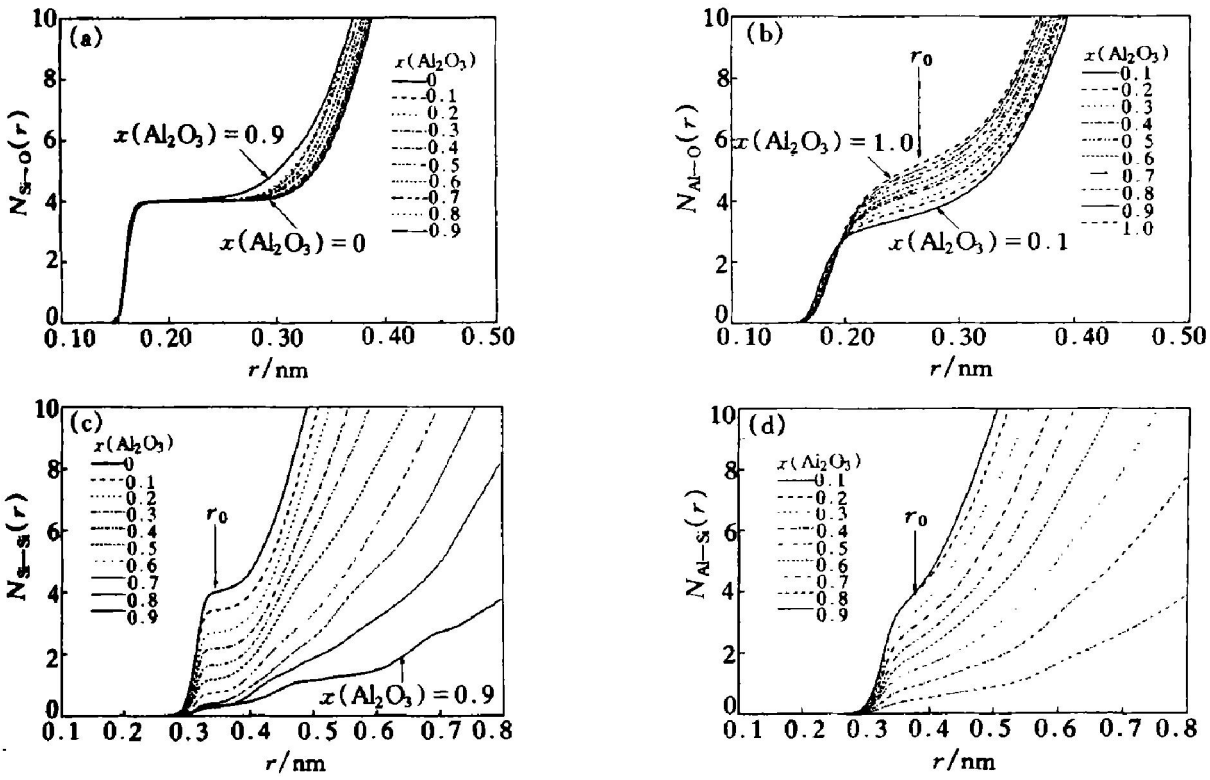

Fig. 4 Coordination Number (CN) with composition
(a) —Si-O; (b) —Al-O; (c) —Si-Si; (d) —Al-Si

From Fig. 5(a), with the decreasing ratio of Si to Si+ Al, CN(Al) increased linearly to 5.2 at pure Al_2O_3 melt (which is higher than that calculated by Poe et al[4]), and CN(Si) had no change, fixed at 4 (supported by the X-ray emission spectroscopic data[21] as presented in the first section). It must be noted the crossing point about Si/(Si+ Al) = 0.5, where CN(Al) is just a little greater than 4. When Si/(Si+ Al) > 0.5, there must come forth the Al (V) and Al(VI) because the CN(Al) is greater than 4. And on the contrary, when Si/(Si+ Al) < 0.5, there should be predominantly Al(IV) and a little Al-

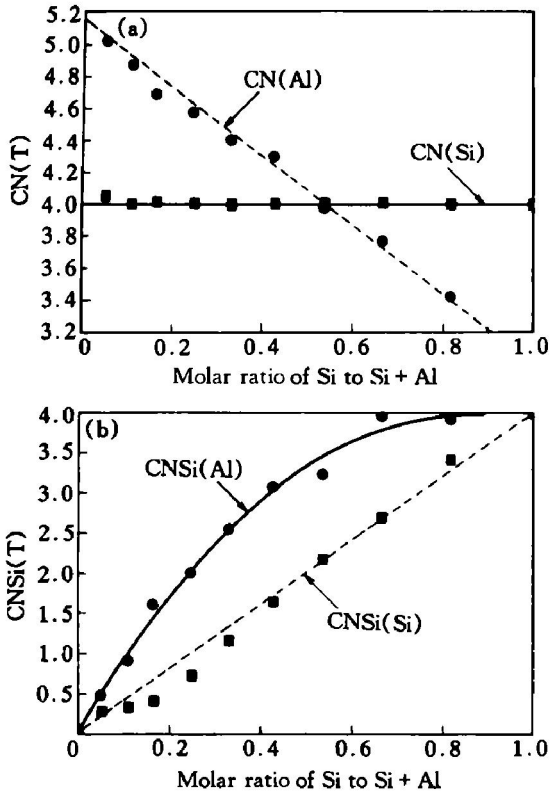

Fig. 5 Relations of coordination numbers CN(T) (a) and CNSi(T) (b) with Si/(Si+ Al)

(Ⅲ). With the increasing content of Al_2O_3, the predominant Al-units changed from tetrahedra to octahedra. This conclusion can be supported by X-ray scattering data[10~22].

Here, CNSi(T) is defined to denote the coordination number of NNN (next-nearest neighbor) Si about T(Si or Al) cation. The relations of CNSi(Si) and CNSi(Al) with Si/(Si+ Al) are shown in Fig. 5(b). When Si/(Si+ Al) is high from 0.7 to 1.0, CNSi(Al) remained 4, which means Al tetrahedra are all surrounded by Si tetrahedra through Al-O-Si bridging oxygen and the Al avoidance principle can be applied to this region just like the results of some literatures[1~3,5,7~10]. But with decreasing Si/(Si+ Al) sequentially, CNSi(Al) almost linearly decreased accompanying with the increase of CN(Al). So, Al-O-Al bridging oxygen inevitably appeared and continued increasing with adding of Al_2O_3 on condition that the system is full-polymerized. Then, the Al avoidance principle can't be maintained any longer. At the meantime, CNSi(Si) is almost linearly related with Si/(Si+ Al), specially when Si/(Si+ Al) > 0.4. When Si/(Si+ Al) is lower than 0.4, the predominant units are not the Si tetrahedra anymore but Al tetrahedra and Al octahedra, it can be imagined that the Si tetrahedra are all immersed in the ocean of Al units. So, CNSi(Si) can not maintain the linear relation with Si/(Si+ Al) anymore. That is also the reason why the peaks and shoulders of $g_{O\text{-}O}(r)$ shown in Fig. 3(c) had a gradual shift along with increasing mole fraction of Al_2O_3. The gradual change from predominantly Si-tetrahedral units to predominantly Al-units and from predominantly Al-tetrahedral ones to predominantly Al-octahedral units is also substantiated by density data of Aksay et al[20].

4 CONCLUSIONS

1) With the potential by combining KA and MATSUMIYA parameters, the results of simulations agree better with the experiments than KA potential and the Si-tetrahedral units in simulated systems become more stable.

2) The average bond length of Si-O in these simulations is within the range of 1.60~ 1.63 Å and becomes smaller from 1.63 Å in sample 0 to 1.60 Å in sample 9 with the increasing content of Al_2O_3. It can be interpreted that the compression brought to the Si-tetrahedra by NNN-Al becomes stronger with increasing alumina composition.

3) The average bond length of Al-O is within the range from 1.77 Å in sample 1 to 1.86 Å in sample 10. It tones in with the coordination number of Al.

4) The coordination number of Si (CN(Si)) are fixed at 4 throughout the entire composition region. But CN(Al) has a linear raise with the addition of alumina. With low content of Al_2O_3 (Si/(Si+ Al) > 0.5), Al mainly locates at the tetrahedral sites which neighbor the Si tetrahedra but avoid the Al tetrahedra. Whereas when Si/(Si+ Al) < 0.5, Al-octahedral units appeared and became predominant gradually.

5) With the increase of Si/(Si+ Al), CNSi(Al) almost linearly increased at first and remained at 4 when Si/(Si+ Al) > 0.7. But CNSi(Si) was reversed and linearly increased when Si/(Si+ Al) > 0.4. So, it can be inferred that Al avoidance principle can only be maintained at low alumina content. With increasing alumina, the principle would be broken gradually.

6) On the condition that the bond and coordination properties of aluminum silicate melts have been understood fully, the next paper will discuss the type of basic units and their distribution.

[REFERENCES]

[1] Mysen B. Role of Al in depolymerized, peralkaline aluminosilicate melts in the systems Li_2O-Al_2O_3-SiO_2, Na_2O-Al_2O_3-SiO_2 and K_2O-Al_2O_3-SiO_2 [J]. Am Mineral, 1990, 75: 120.

[2] McMillan P, Piriou B, Navrotsky A. A raman spectroscopic study of glasses along the joins silica-calcium aluminate, silica-sodium aluminate, and silica-potassium aluminate [J]. Geochim et Coschim Acta, 1982, 46: 2021.

[3] Daniel J S, Frank J S. In-situ high-temperature Raman spectroscopic studies of aluminosilicate liquids [J]. Phys Chem Minerals, 1995, 22: 74.

[4] Poe B T, McMillan P T, Angell C A, et al. Al and Si coordination in SiO_2-Al_2O_3 glasses and liquids: a study by NMR and IR spectroscopy and MD simulations [J]. Chem Geo, 1992, 96: 333.

[5] Miura Y, Matsumoto S, Nanba T, et al. X-ray photoelectron spectroscopy of sodium aluminosilicate glasses [J]. Phys Chem Glasses, 2000, 41(1): 24.

[6] Merzbacher C I, Sherrif B L, Hartman J S, et al. A high-resolution ^{29}Si and ^{27}Al NMR study of alkaline earth aluminosilicate glasses [J]. J Non-Crystal Solids, 1990, 124: 194.

[7] Engelhardt G, Nofz M, Forkel K, et al, Structural studies of calcium aluminosilicate glasses by high resolution solid state ^{29}Si and ^{27}Al magic angle spinning nuclear magnetic resonance [J]. Phys Chem Glasses, 1985, 26(5): 157.

[8] Nofz M, Stösser R, Wihsmann F G, et al. Paramagnetic centres in glasses of the system CaO-Al_2O_3-SiO_2 [J]. Phys Chem Glasses, 1990, 31(2): 57.

[9] Nofz M, Forkel K, Wihsmann F G, et al. Cluster analysis of ^{29}Si nuclear magnetic resonance spectra of aluminosilicate glasses [J]. Phys Chem Glasses, 1989, 30(2): 46.

[10] Oestrike R, Yang W H, Kirkpatrick R J, et al. High-resolution ^{23}Na, ^{27}Al, and ^{27}Si NMR spectroscopy of framework aluminosilicate glasses [J]. Geochim et Coschim Acta, 1987, 51: 2199.

[11] Himmel B, Weigelt J, Gerber T H, et al. Structure of calcium aluminosilicate glasses: wide angle X-ray scattering and computer simulation [J]. J Non-Crystal Solids, 1991, 136: 27.

[12] Morikawa H, Miwa S H I, Miyake M, et al. Structural analysis of SiO_2-Al_2O_3 glasses [J]. J Am Ceram Soc, 1982, 65(2): 78.

[13] Huff N T, Demiralp E, Cagin T, et al. Factors affecting molecular dynamics simulated vitreous silica structures [J]. J Non-Crystal Solids, 1999, 253: 133.

[14] Kieffer J, Angell C A. Structural incompatibilities and liquid-liquid phase seperation in molten binary silicates: A computer simulation [J]. J Chem Phys, 1989, 90(9): 4982.

[15] Athanasopoulos D C, Garofalini S H. Effect of absorption on the surface structure of sodium alumino-silicate glasses: a molecular dynamics simulation [J]. Surface Science, 1992, 273: 129.

[16] Scamehorn C A, Angell C A. Viscosity-temperature relations and structure in fully polymerized aluminosilicate melts from ion dynamics simulations [J]. Geochim Cosmochim Acta, 1991, 55: 721.

[17] Matsumiya T, Nogami A, Fukuda Y. Application of molecular dynamics to analyses of refining slags [J]. ISIJ International, 1993, 33(1): 210.

[18] Stein D J, Spera F J. Molecular dynamics simulations of liquids and glasses in the system $NaAlSiO_4$-SiO_2: methodology and melt structure [J]. Am Mineral, 1995, 80: 417.

[19] Hatalova B, Liska M. The bimodality in the SiOSi bond angle distribution in simulated sodium silicate systems [J]. J Non-Crystal Solids, 1992, 146: 218.

[20] Loewenstein W. The distribution of aluminum in the tetrahedra of silicates and alumivates [J]. Am Miner, 1954, 39: 92.

[21] Hanada T, Soga N. Coordination and bond character of silicon and aluminum ions in amorphous thin films in the system SiO_2-Al_2O_3 [J]. Commu of Am Ceram Soc, 1982, 6: C-84.

[22] Aksay I A, Pask J A. Densities of SiO_2-Al_2O_3 melts [J]. J Am Ceram Soc, 1979, 62(7/8): 332.

(Edited by LONG Huai-zhong)